


Research Paper

Analysis of the Vehicle Engine Misfires using Frequency-Domain Approaches at Various RPMs with ADXL1002 Accelerometer

Muhammad AHSAN^{(1)*} , Dariusz BISMOR⁽¹⁾, Paweł FABIŚ⁽²⁾⁽¹⁾ Department of Measurements and Control Systems, Silesian University of Technology
Gliwice, Poland⁽²⁾ Faculty of Transport and Aeronautical Engineering, Department of Road Transport
Silesian University of Technology
Katowice, Poland*Corresponding Author e-mail: ahsanmuhammad@aol.com/Muhammad.Ahsan@polsl.pl

(received December 31, 2023; accepted May 13, 2024; published online xxx)

Vehicle engine vibration signals acquired using MEMS sensors are crucial in the diagnosis of engine malfunctions, notably misfires due to unwanted signals and external noises in the recorded vibration dataset. In this study, the ADXL1002 accelerometer interfaced with the Beaglebone Black microcontroller is employed to capture vibration signals emitted by the vehicle engine across various operational states, including unloaded, loaded, and misfire conditions at 1500 RPMs, 2500 RPMs, and 3000 RPMs. In conjunction with the acquisition of this raw vibration data, frequency-domain signal processing techniques are employed to meticulously analyze and diagnose the distinct signatures of misfire occurrences across various engine speeds and loads. These techniques encompass the fast Fourier transform (FFT), envelope spectrum (ES), and empirical mode decomposition (EMD), each tailored to discern and characterize the nuanced vibration patterns associated with misfire events at different operational conditions.

Keywords: ADXL1002 accelerometer; MEMS sensors; vehicle engine vibration; misfire condition; fast Fourier transform; envelope spectrum; empirical mode decomposition.

Copyright © 2024 The Author(s).
This work is licensed under the Creative Commons Attribution 4.0 International CC BY 4.0
(<https://creativecommons.org/licenses/by/4.0/>).

1. Introduction

Misfire, a persistent issue in vehicle engines, disrupts the harmonious sequence of combustion. Its prevalence is striking, causing substantial hurdles in engine performance and reliability, as highlighted in the research conducted by *HMIDA et al. (2021)*. This fault, defined by the inability of a cylinder to ignite its air-fuel mixture correctly, extends its impact across multiple domains. Recognizing and remedying misfires is of paramount importance in automotive engineering. *NAVEEN VENKATESH et al. (2022)* underscore the criticality of accurate detection and timely resolution of this issue. Essentially, mitigating misfires is not just about fixing a glitch; it is about preserving the efficiency and ecological integrity of vehicle engines.

Various contemporary techniques have emerged as effective means to pinpoint engine misfire faults, show-

ing the innovative strides in this field. For instance, one approach capitalizes on the ionic current (I.C.) presented at spark plug electrodes, leveraging them as sensors to detect misfiring cylinders. Studies referenced by *WANG et al. (2022)* and *KUMANO et al. (2020)* delve into this method, illustrating how monitoring changes in ionic current during engine operation offers insights into discerning misfiring events.

Another notable method involves monitoring the exhaust gas temperature at a reduced sampling rate. *TAMURA et al. (2011)* shed light on this technique, emphasizing its utility in detecting misfires within internal combustion engines. By scrutinizing irregular temperature fluctuations in the exhaust gas, this approach identifies deviations that serve as reliable indicators of misfiring occurrences.

Meanwhile, exploring the combustion characteristics and misfire mechanisms in passive pre-chamber

direct-injection gasoline engines presents a specialized avenue. ZHOU *et al.* (2023) contributed to this area, focusing on understanding the intricate combustion behavior and misfire processes unique to engines employing passive pre-chamber technology for gasoline direct injection. This method delves into the specificities of how these engines operate and experience misfire events, offering insights crucial for their optimization.

Moreover, a holistic approach to misfire detection in aircraft engines involves integrating both linear signal analysis for pattern recognition and non-linear methods. The study highlighted by SYTA *et al.* (2021) underscores this comprehensive strategy, demonstrating how combining diverse analytical techniques ensures a robust and multifaceted approach to identifying misfire incidents.

However, vibration signals offer an easy measurable method without affecting engine function (HMIDA *et al.*, 2021; SHARMA *et al.*, 2014). The examination of vehicle engine vibrations serves as a profound gateway to deciphering the inner workings of an internal combustion engine. These vibrations intricate in their composition, encapsulate a wealth of data pertaining dynamical performance of the engine (SHARMA *et al.*, 2014; DU *et al.*, 2021). The scrutiny of these vibration signals holds immeasurable significance as a diagnostic tool, particularly in isolating specific engine misfires (HMIDA *et al.*, 2021; SHARMA *et al.*, 2014). The majority of research has focused on utilizing various sensors like accelerometers, acoustic sensors, and knock sensors to measure vibration signals (FIRMINO *et al.*, 2021; TAO *et al.*, 2019), yielding satisfactory outcomes and broad implementation in monitoring machinery conditions like pumps, ball bearings, and gearboxes (AHSAN, BISMOR, 2022; AHSAN *et al.*, 2023). Nevertheless, these methods encounter challenges in assessing specific conditions of vehicle engines due to the nonstationary nature of the measured signals when conventional analysis techniques are applied.

A diverse array of sensors contributes to the comprehensive analysis of engine vibrations (BISMOR, 2019). Comparative studies in the literature have examined a piezoelectric acceleration sensor specifically designed for engine and transmission vibration measurement against commercially produced accelerometer signals (BISMOR, 2019; GÜL *et al.*, 2021). Existing literature consistently demonstrates that engine vibration intensity correlates with increased engine speed and load variations (YAŞAR *et al.*, 2019).

The renowned piezoelectric sensors boast remarkable sensitivity in detecting high-frequency vibrations, efficiently translating mechanical impulses into electrical signals. Conversely, MEMS sensors, particularly accelerometers, stand out for their adaptability and precision in registering vibrations across various axes (LI *et al.*, 2020; AHSAN, BISMOR, 2023). Despite higher noise levels compared to piezoelectric sensors, the

compact size, affordability, and expansive capacity of MEMS sensors to measure a broad spectrum of vibration frequencies make them particularly suited for the intricate demands of engine monitoring and diagnostic purposes. These attributes collectively render MEMS sensors highly adept for addressing the multifaceted needs of engine analysis and diagnostics.

MEMS sensors, despite their versatility, encounter two prominent challenges in the realm of engine vibration analysis (BISMOR, 2019). Firstly, the vibration signals obtained through MEMS sensors often exhibit higher levels of noise compared to their piezoelectric counterparts. This discrepancy in noise levels stems from several factors rooted in the construction and operating principles of MEMS sensors. The miniaturized size of MEMS sensors, while advantageous for their widespread applicability and cost-effectiveness, can also make them more susceptible to environmental interferences and internal noise generated within the sensor itself. Additionally, the fabrication process and material composition of MEMS sensors may introduce inherent noise that affects the accuracy of vibration signal acquisition. Literature and academic research underscore the significance of addressing these noise factors in MEMS sensors to enhance their performance and reliability in capturing vibration data accurately (ROSSI *et al.*, 2023). Secondly, MEMS sensors necessitate meticulous calibration to ensure synchronization between the reference frequency and the recorded frequency of vibration signals (AHSAN, BISMOR, 2023). Achieving this synchronization is critical for precise analysis and interpretation of the acquired data.

The research endeavors in this study encompass a comprehensive analysis of engine vibrations using the MEMS sensor technology, specifically focusing on the ADXL1002 accelerometer paired with the Beaglebone Black microcontroller. The ADXL1002 accelerometer interfaced with the BeagleBone Black aims to minimize costs compared to pricier piezoelectric sensors while ensuring efficient data acquisition and analysis. This cost-effective approach enhances access to reliable vibration data crucial for accurately detecting misfires at diverse engine operating speeds. A critical precursor to this investigation involves the calibration of the ADXL1002 accelerometer with the Beaglebone Black setup. Calibration procedures were meticulously conducted utilizing the vibrator and signal generator to ensure accuracy and reliability in capturing vibration data. Detailed insights into this calibration process are extensively documented in the conference paper (AHSAN, BISMOR, 2023), providing a foundation for the subsequent experimentation and analysis conducted in this research. The primary objective is to capture vibration signals emitted by the vehicle engine across various operational states, including unloaded, loaded, and misfire conditions at dif-

ferent RPMs. In conjunction with the acquisition of this raw vibration data, frequency-domain signal processing techniques are employed to meticulously analyze and diagnose the distinct signatures of misfire occurrences across varying engine speeds and loads. These techniques encompass the fast Fourier transform (FFT), envelope spectrum (ES), and empirical mode decomposition (EMD), each tailored to discern and characterize the nuanced vibration patterns associated with misfires at different operational conditions. This multifaceted approach aims to enhance the diagnostic capabilities for detecting and differentiating misfire events, contributing to a more robust understanding of engine performance under diverse circumstances.

2. Materials and methods

This section delineates the developed prototype of the ADXL1002 accelerometer interfaced with the Beaglebone Black and the meticulous calibration process undertaken to ensure its accuracy and reliability in capturing vibration data. Additionally, it details the methodology employed in recording vibration data from the vehicle engine across diverse operational conditions, encompassing normal, loaded, and misfire scenarios at various RPMs, and the acquired data is presented. This section also encompasses an in-depth description of the different signal processing techniques utilized for diagnosing misfire conditions, outlining the specific methodologies employed in the analysis of the acquired vibration data.

2.1. Calibration of ADXL1002 accelerometer

The ADXL1002 is a high-performance accelerometer that measures acceleration in a single in-plane axis. It has an analog output that is proportional to the supply voltage and a linear frequency response range from DC to 11 kHz. It also has a low noise density of $25 \mu\text{g}/\sqrt{\text{Hz}}$ and a high resonant frequency of 21 kHz, which make it suitable for vibration and shock sensing applications. The ADXL1002 has a self-test function, a sensitivity stability of 5% over temperature, and a low cross axis sensitivity of $\pm 1\%$. It operates from a single supply and has a low power consumption of 1.0 mA. It also has a standby mode that reduces power consumption and allows fast recovery. The ADXL1002 can withstand temperatures from -40°C to $+125^\circ\text{C}$ and comes in a small $5 \text{ mm} \times 5 \text{ mm} \times 1.80 \text{ mm}$ LFCSP package. It is RoHS compliant and meets the environmental standards for electronic devices (Analog Devices, n.d.).

The calibration protocol for the ADXL1002 accelerometer involves a systematic series of steps designed to ensure the accuracy and reliability of data collection (AHSAN, BISMOR, 2023). Initial setup includes interfacing the accelerometer with the Beagle-

Bone Black microcontroller, establishing robust communication protocols between the two systems, laying the groundwork for subsequent calibration stages.

The experimental setup for calibration, detailed in Fig. 1, incorporates essential components such as a signal generator, power amplifier, vibration exciter, measuring amplifier, the MEMS accelerometer (ADXL1002), and the BeagleBone Black microcontroller, all integral to the calibration procedure. In the experimental setup, sinusoidal signals spanning different frequencies were generated by the function generator, initiating the attached vibration exciter to induce vertical vibrations. An ADXL1002 accelerometer, interfaced with the BeagleBone Black, captured and recorded these induced vibrations.

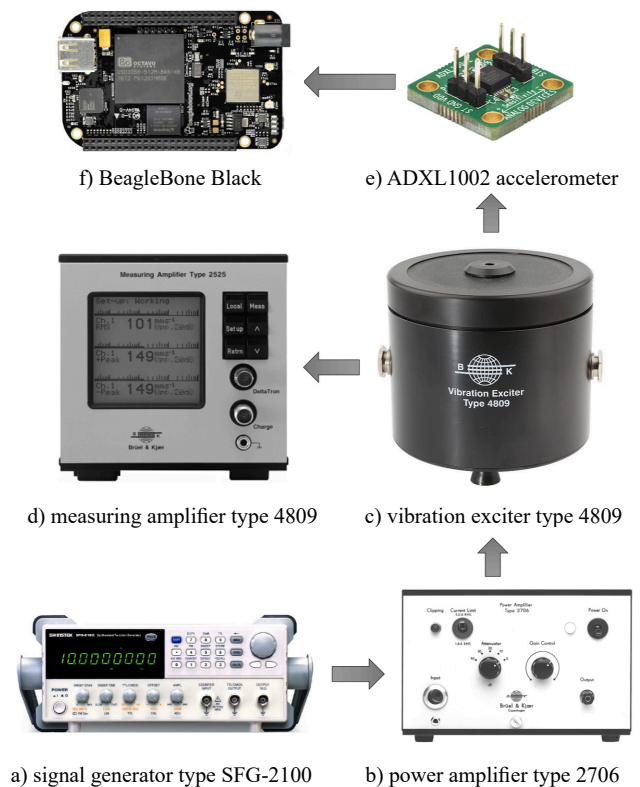


Fig. 1. Controlled environment setup for ADXL1002 accelerometer calibration: a) signal generator type SFG-2100; b) power amplifier type 2706; c) vibration exciter type 4809; d) measuring amplifier type 2525; e) ADXL1002 accelerometer; f) BeagleBone Black.

The FFT was utilized to analyze the time-domain vibration signals produced by the vibration exciter, computing the recorded frequencies and subsequently comparing them with the reference frequencies of the input signal to the vibration exciter. Remarkably, the plot depicted in Fig. 2 reveals a linear relationship between the reference and measured frequencies, affirming the efficiency of the ADXL1002 accelerometer and reliable detection of input frequencies.

Following the frequency comparison analysis, the sensitivity of the ADXL1002 accelerometer to recorded

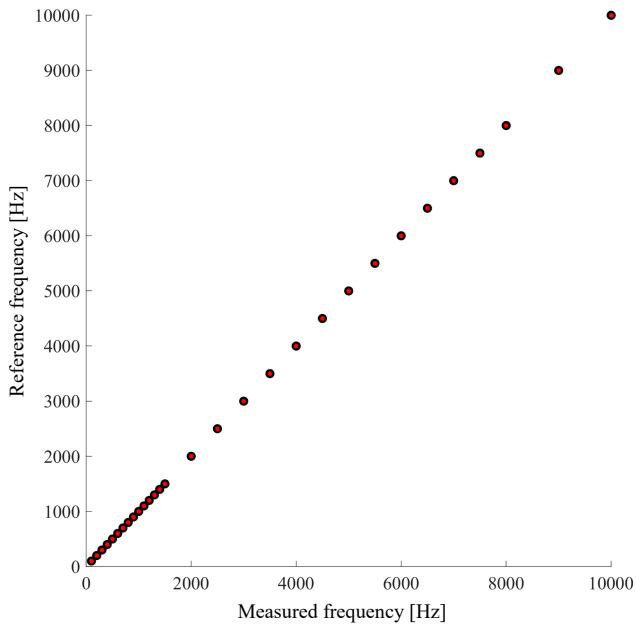


Fig. 2. Comparison of reference and computed frequencies using FFT analysis.

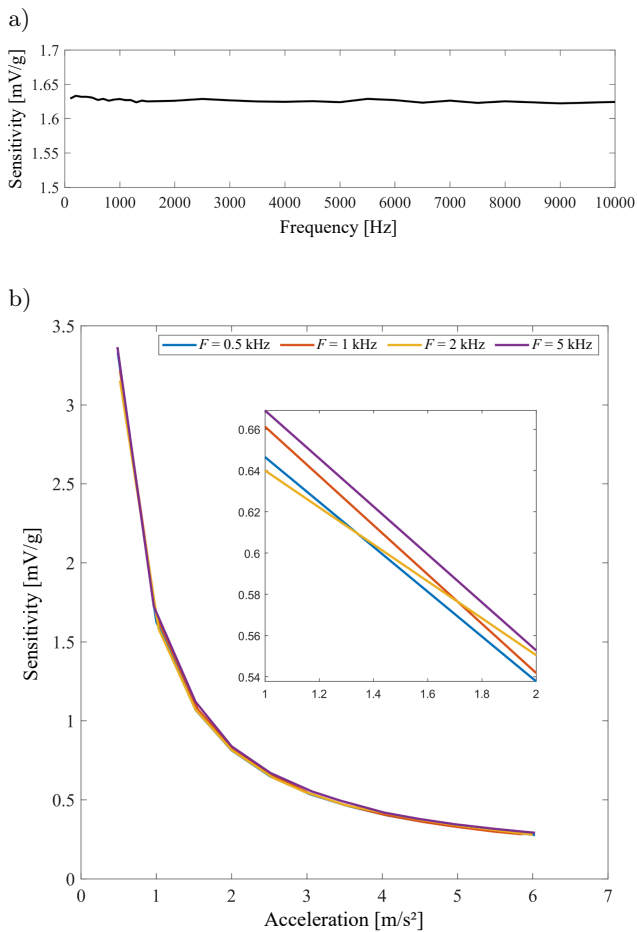


Fig. 3. Sensitivity analysis of ADXL1002 accelerometer: a) sensitivity plotted against frequencies showcasing consistent sensitivity across frequency ranges; b) sensitivity variation with gravitational forces, highlighting an inverse relationship between sensitivity and gravitational levels.

vibration signals was determined using the following equation:

$$S_i = \frac{\text{RMS}(v(f_i))}{g_i}, \quad (1)$$

where $v(f_i)$ represents the time-domain vibration signal at a specific frequency f_i with $i = 1, 2, 3, \dots, k$, g_i denotes the acceleration of the vibration signals, and $\text{RMS}(\cdot)$ denotes the root-mean-square of the signal. This sensitivity analysis was depicted in Fig. 3a, demonstrating consistent sensitivity levels across various frequency ranges. Additionally, Fig. 3b illustrates the inverse proportionality between sensitivity and gravitational force, indicating that higher gravitational levels resulted in reduced sensitivity.

Utilizing the developed prototype of the ADXL1002 accelerometer interfaced with the BeagleBone Black, the calibration process lays the foundation for advanced applications in misfire detection within vehicle engine vibration data.

2.2. Vibration dataset of vehicle engine using ADXL1002 accelerometer

Figure 4 visually depicts the placement of the accelerometer on the vehicle engine, illustrating its positioning for data capture purposes. The vehicle engine vibration dataset given in Table 1 offers a structured overview of engine conditions across various RPMs, loads, and misfire occurrences. Each entry in the table corresponds to a specific engine scenario, denoted by RPM (revolutions per minute), load intensity, and misfire status. The dataset captures instances across different RPMs, including 1500, 2500, and 3000, coupled with load conditions ranging from no load to half load and full load. Moreover, the dataset signifies whether a misfire was present or absent in each specific scenario. This dataset serves as a comprehensive representation of engine performance variations under different operational settings, allowing for in-depth analysis and exploration of how RPM, load, and misfire interrelate within the context of vehicle vibrations.

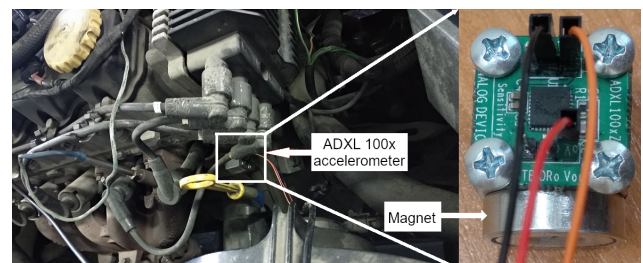


Fig. 4. Placement of ADXL1002 accelerometer on vehicle engine for vibration data collection.

To further elucidate the engine vibration dataset captured through the ADXL1002 accelerometer, a representation in the time domain is crucial for visual

Table 1. Vehicle engine vibration dataset.

RPM	Frequency [Hz]	Load	Misfire
1500	25	no load	no misfire
3000	50	no load	no misfire
1500	25	half load	no misfire
1500	25	full load	no misfire
2500	41.667	half load	no misfire
2500	41.667	full load	no misfire
3000	50	half load	no misfire
3000	50	full load	no misfire
1500	25	half load	misfire
1500	25	full load	misfire
2500	41.667	half load	misfire
2500	41.667	full load	misfire
3000	50	half load	misfire
3000	50	full load	misfire

comprehension. The selected vibration signals, depicted in Fig. 5 showcase the temporal characteristics of engine vibrations across distinct operational states. These signals, plotted against time, offer a direct insight into the fluctuations and patterns within the recorded vibrations during various engine conditions at 3000 RPMs, such as load levels, and misfire occurrences.

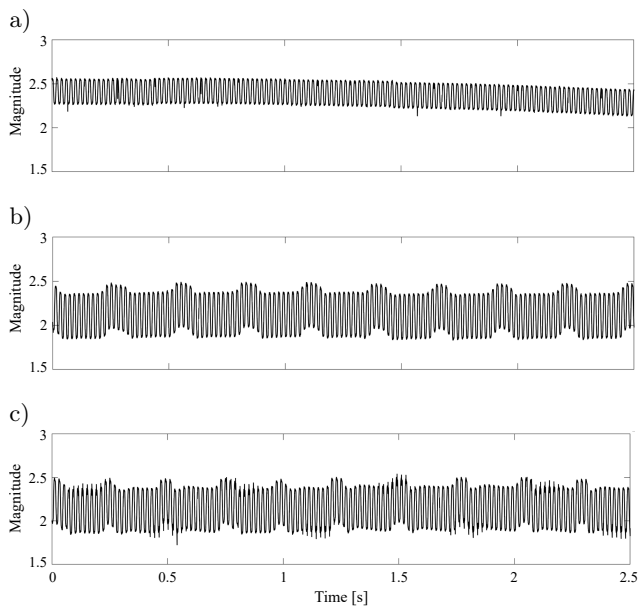


Fig. 5. Engine vibration signals at 3000 RPMs under varied load conditions and misfire scenarios: a) unloaded without misfire condition; b) loaded without misfire condition; c) loaded with misfire condition.

2.3. Frequency-domain approaches for misfire diagnoses

Misfires in a vehicle engine indeed have a tangible impact on the vibration signal's spectrum. These dis-

ruptions occur when the typical firing sequence of the engine cylinders is disturbed, resulting in irregularities in the vibration pattern. The introduction of additional frequency components, particularly around the harmonics or multiples of the engine's firing frequency, is a hallmark of misfires. Consequently, these irregular firing patterns lead to distinct spikes or alterations in the spectral content of the vibration signal. Detecting these deviations becomes pivotal for diagnostics and maintenance, necessitating advanced signal processing techniques capable of differentiating between load-induced alterations and the presence of misfires within the intricate vibration signals generated during engine operation.

2.3.1. FFT approach for misfire detection

Utilizing the FFT in the misfire and engine analysis involves decomposing vibration signals into their fundamental frequency components, unveiling spectral patterns inherent within the signals (LIN, YE, 2019).

The FFT algorithm computes the discrete Fourier transform (DFT) efficiently. Mathematically, the DFT of a discrete-time function $f(n)$ can be represented as follows (LIN, YE, 2019):

$$F(k) = \sum_{n=0}^{N-1} f(n)e^{-i2\pi kn/N}, \quad (2)$$

where $F(k)$ denotes the complex values within the frequency domain at a specific index k . This complex value represents the transformed signal's amplitude and phase at a particular frequency component. On the other hand, $f(n)$ signifies the discrete-time signal in the time domain at a distinct index n . The variable N represents the total count of samples constituting the time-domain signal. The term $e^{-i2\pi kn/N}$ is a complex exponential expression encapsulating the phase shift and frequency of individual components within the signal.

2.3.2. Envelope spectrum approach for misfire detection

The computation of the ES stands as an essential method to discern nuanced variations induced by both load and misfire events. This technique entails the extraction of the signal's envelope, thereby highlighting alterations in the overall vibration behavior attributed to changes in load or misfires. This approach furnishes accurate diagnostic insights into the operational state of the engine, pinpointing specific modifications in the vibration patterns influenced by varying loads or misfire occurrences (AHSAN, BISMOR, 2022).

The ES represents the amplitude of specific frequency components within a signal $f(n)$. Mathematically, the computation of the ES involves obtaining the

magnitude spectrum of the positive frequency components obtained from the signal's FFT. The equation for the ES for a signal $f(n)$ can be expressed as $ES(k)$:

$$ES(k) = \text{FFT}_{\text{positive}}(k), \quad (3)$$

where the symbol $ES(k)$ signifies the ES at a specific index k within the frequency domain representation. Meanwhile, $\text{FFT}_{\text{positive}}(k)$ represents the positive frequency components extracted from the FFT computation conducted on the signal. The operation $\|\cdot\|$ denotes the magnitude operation, commonly known as the absolute value operation. This mathematical operation retrieves the amplitude information from the positive frequency components derived through the FFT process, allowing for the extraction of the ES showcasing the amplitudes of distinct vibration frequencies within the signal.

In essence, the ES is derived by taking the absolute values of the positive frequency components obtained through the FFT process of the signal $f(n)$. This representation highlights the amplitudes of selected vibration frequencies within the signal.

2.3.3. EMD approach for misfire detection

The EMD serves as an invaluable tool in analyzing the intricacies of non-linear and non-stationary signals, offering a means to disentangle them into components of varying resolutions (LIU *et al.*, 2021). The process of EMD involves several steps. Initially, extrema, comprising local maxima and minima points, are identified within the signal $f(n)$. Subsequently, upper and lower envelopes are formed by connecting these extrema points. The mean signal, obtained by calculating the mean of the upper and lower envelopes, is then subtracted from the original signal $f(n)$ to derive the first intrinsic mode function (IMF). This process is iteratively applied to the obtained IMF, treating it as the new signal in each iteration, until specific convergence or stopping criteria are met. The iterative nature of EMD allows it to adapt to the characteristics of the input signal, resulting in the successive extraction of IMFs that collectively represent the signal's intrinsic oscillatory modes.

Misfires within the engine introduce additional, unfamiliar frequencies and harmonics into these vibration signals, intensifying the intricacy of the diagnostic process. To dissect and interpret these signals accurately, advanced signal processing techniques are crucial in distinguishing, analyzing, and understanding the new frequency components attributed to misfires. EMD, by its inherent nature, offers a potent means to handle these challenges. Its ability to effectively decompose signals into varying resolutions aligns with the demands posed by the intricate nature of vibration signals, especially in the presence of misfires. Thus, EMD emerges as a suitable technique to disentangle and in-

terpret these complex signals, facilitating a deeper understanding of the new frequency components introduced by misfires and aiding in precise engine diagnostics.

3. Results and discussion

Figure 6 illustrates the FFT representations of vibration signals at 1500 RPMs under varied load conditions and misfire scenarios: unloaded without misfire, loaded without misfire, and loaded with misfire. Notably, the FFT demonstrates harmonic frequency components within the loaded vibration signals, yet fails to reveal the 1500 RPM (25 Hz) frequency component in the presence of a misfire, as indicated in Fig. 6.

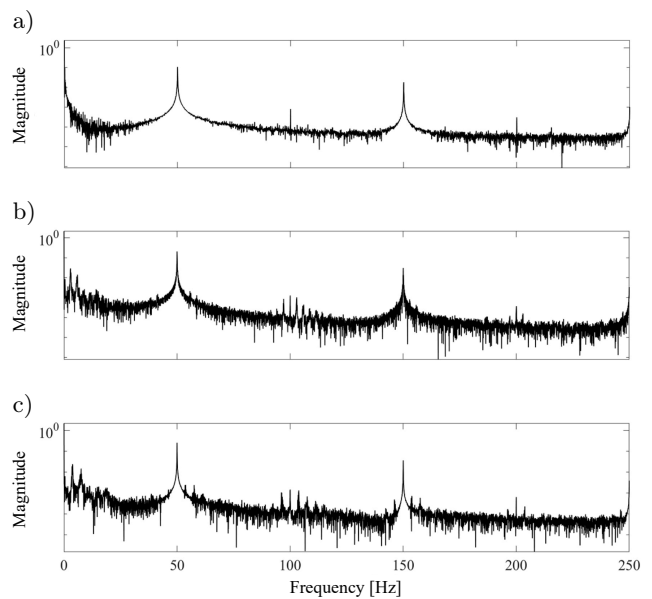


Fig. 6. FFT of raw vibration signals at 1500 RPMs under varied load conditions and misfire scenarios: a) unloaded without misfire condition; b) loaded without misfire condition; c) loaded with misfire condition.

Vibration signals recorded from vehicle engines via MEMS sensors, like the ADXL1002 accelerometer, often encompass unwanted frequencies that deteriorate the signal-to-noise ratio. During engine misfires, the power associated with the misfire frequency substantially diminishes, rendering it imperceptible within the FFT representation (Fig. 6).

However, misfires within the engine generate discernible periodic impacts in the time-domain vibration signals, as depicted in Fig. 5. ES analysis serves as a potent frequency-domain signal processing tool capable of highlighting misfire frequencies within vibration signals. Figure 7 showcases the ES representations of loaded signals without misfires, at 1500 RPMs and 2500 RPMs. These representations underscore the effectiveness of ES in discerning the absence of misfires

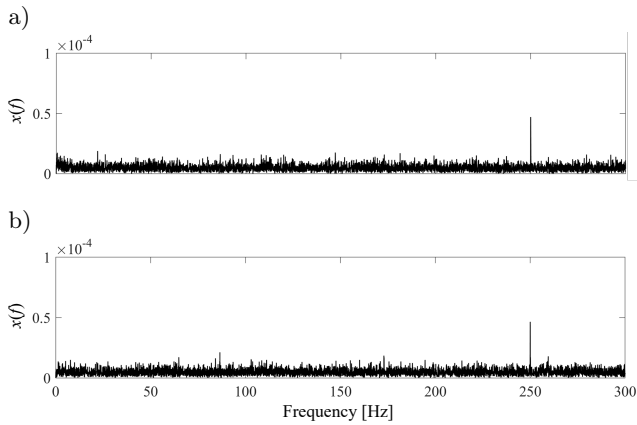


Fig. 7. Envelope spectrum of raw vibration signals at different RPMs under loaded and no misfire conditions: a) 1500 RPMs; b) 2500 RPMs.

within the engine, thereby exhibiting a clear spectral output.

Moreover, Fig. 8 illustrates the misfire frequency at 1500 RPMs (25 Hz) for both half load and full load conditions. Similarly, Figs. 9 and 10 showcase the ES representations at 2500 RPMs (41.667 Hz) and 3000 RPMs (50 Hz), correspondingly. Specifically, Fig. 9a displays ES for half load, while Fig. 9b present ES for full load. Similarly, Fig. 10a exhibits ES for half load, and Fig. 10b showcases ES for full load, illustrating the frequency components pertinent to their respective misfire frequencies.

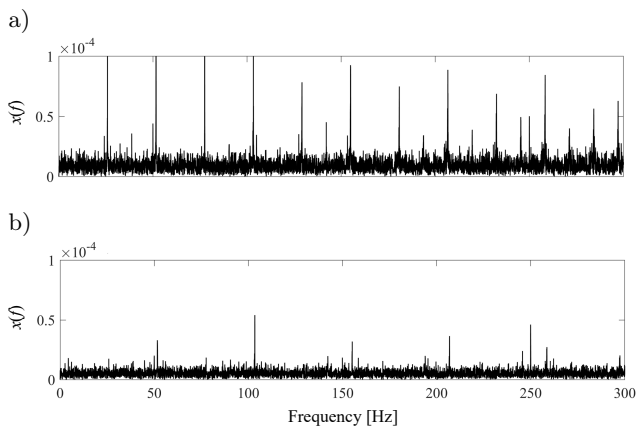


Fig. 8. Envelope spectrum of raw vibration signals at 1500 RPMs under loaded and misfire conditions: a) half load; b) full load.

The observations and discussions from the preceding analysis suggest that the ES offers enhanced proficiency in detecting misfires compared to the FFT applied to the raw vibration signals acquired using the ADXL1002 accelerometer. The diagnosis of misfires in vehicle engines utilizing the ADXL1002 accelerometer revolves around identifying periodic impulses. Upon misfire detection, requisite measures for periodic main-

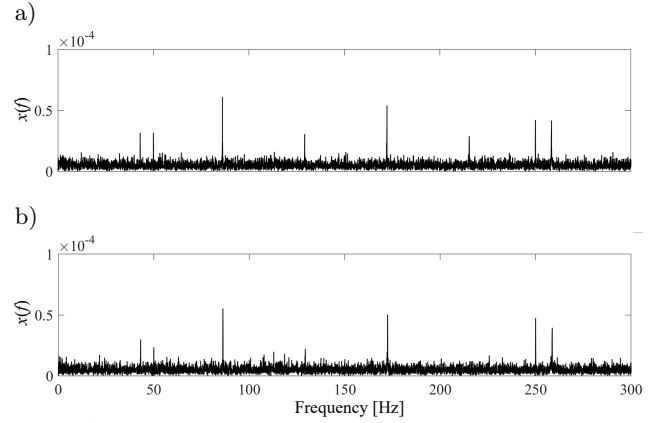


Fig. 9. Envelope spectrum of raw vibration signals at 2500 RPMs under loaded and misfire conditions: a) half load; b) full load.

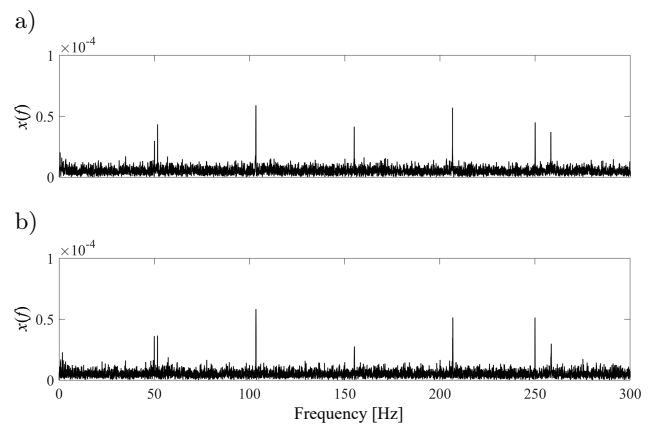


Fig. 10. Envelope spectrum of raw vibration signals at 3000 RPMs under loaded and misfire conditions: a) half load; b) full load.

tenance are undertaken. However, this task poses challenges due to the inherent characteristics of low signal-to-noise ratio and interference from unwanted external signals, as evidenced in the FFT results depicted in Fig. 6.

Figures 11 and 12 illustrate the IMF components pertaining to loaded conditions at 2500 RPMs and 3000 RPMs, respectively. Specifically, Fig. 11 displays the IMF components at 2500 RPMs for the loaded condition without any misfires, while Fig. 12 showcases the IMF components at 3000 RPMs under loaded conditions with misfires.

Figure 13 exhibits the FFT analysis conducted on the first IMF extracted from vibration signals observed at 1500 RPMs, 2500 RPMs, and 3000 RPMs, accounting for both half load and full load conditions. In Figs. 13a and 13b, the display illustrates the presence of the misfire frequency at 1500 RPMs (25 Hz), accompanied by discernible side harmonic frequency components, all stemming from the combined influence of misfires and consistent load conditions – either half load or full load.

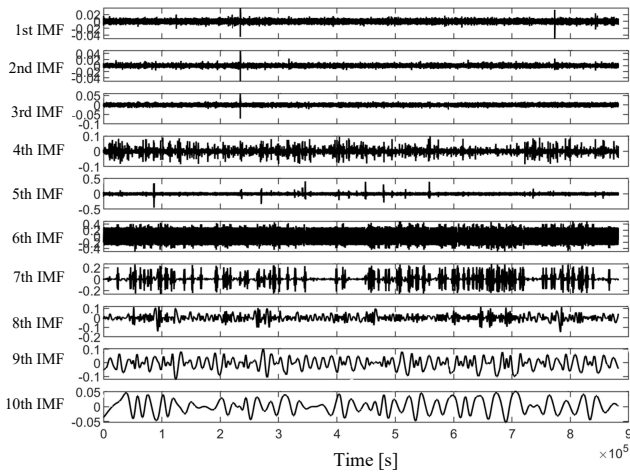


Fig. 11. EMD of vibration signal at 2500 RPMs under loaded and without misfire condition.

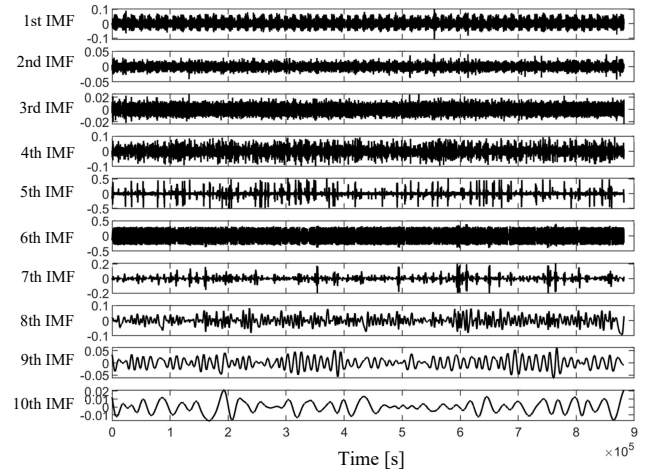


Fig. 12. EMD of vibration signal at 3000 RPMs under loaded and misfire condition.

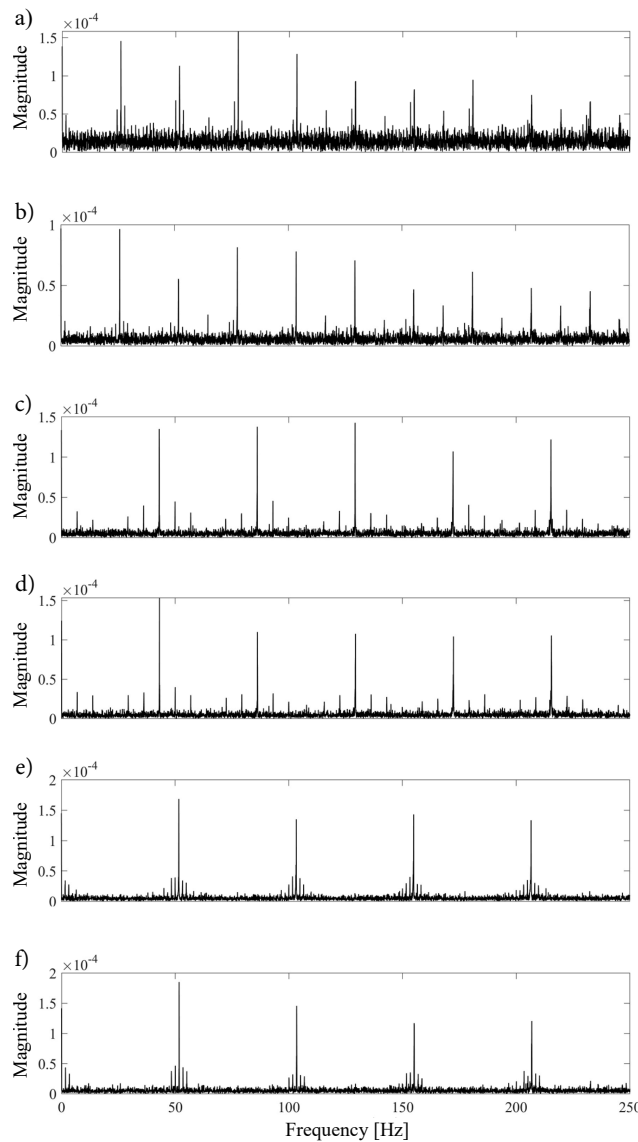


Fig. 13. FFT of the first IMF at different RPMs under loaded conditions and misfire scenarios: a) 1500 RPMs with half load; b) 1500 RPMs with full load; c) 2500 RPMs with half load; d) 2500 RPMs with full load; e) 3000 RPMs with half load; f) 3000 RPMs with full load.

Similarly, Figs. 13c and 13d delineate the 42 Hz misfire frequency, while Figs. 13e and 13f showcase the 50 Hz misfire frequency, specifically identifiable at distinct engine speeds. This analysis, applied to the first IMF, significantly reduces unwanted signals inherent in raw vibration data, offering a more refined representation compared to the observations depicted in Fig. 6.

4. Conclusions

This research highlights the vital role of MEMS sensors, notably the ADXL1002 accelerometer interfaced with the Beaglebone Black microcontroller, in diagnosing complex engine malfunctions. Specifically, it focuses on identifying misfires within intricate vibration datasets. The use of these sensors is crucial in efficiently detecting misfires and other engine irregularities.

The calibration process, meticulously detailed in a previous work (AHSAN, BISMOR, 2023), stands as a fundamental aspect of this study. This calibration ensured precision and reliability in capturing vibration data, serving as a solid foundation for subsequent experiments and analyses.

In this research, the primary objective was to record vibration signals across diverse operational scenarios, encompassing unloaded, loaded, and misfire conditions at varying RPMs. The vehicle engine was equipped with the ADXL1002 accelerometer, and vibration data were systematically recorded under distinct conditions: at 1500 RPMs, 2500 RPMs, and 3000 RPMs. The recorded scenarios included unloaded without misfire, loaded without misfire, and loaded with misfire conditions. Subsequently, the collected data was presented and analyzed in both the time-domain and the frequency-domain to visualize the effects of misfires and varying loads on vibration signals.

Additionally, this involved the application of advanced frequency-domain signal processing techniques such as FFT, ES, and EMD. These methods were carefully designed to distinguish distinctive patterns signifying engine misfires, specifically when considering diverse engine RPMs and loads. This strategic approach substantially amplified our capability to diagnose and understand potential engine issues. The efficiency of applying FFT directly to the raw vibration data was hindered by the presence of unwanted signals and external noises, making misfire detection challenging. To address this issue, EMD was employed to decompose the vibration signal into distinct frequencies. Subsequently, FFT was applied to the first IMF to pinpoint the misfire frequency variations at different RPMs. This method proved effective in diagnosing misfire frequencies within the vibration signals obtained through the use of the ADXL1002 accelerometer in the vehicle engine. Furthermore, it not only enabled the precise

identification of misfires but also provided intricate insights into the precise vibrational characteristics associated with varying engine conditions.

References

- AHSAN M., BISMOR D. (2022), Early-stage fault diagnosis for rotating element bearing using improved harmony search algorithm with different fitness functions, *IEEE Transactions on Instrumentation and Measurement*, **71**: 1–9, doi: [10.1109/TIM.2022.3192254](https://doi.org/10.1109/TIM.2022.3192254).
- AHSAN M., BISMOR D. (2023), Calibration of a high sampling frequency MEMS-based vibration measurement system, [in:] Pawelczyk M., Bismor D., Ogonowski S., Kacprzyk J. [Eds.], *Advanced, Contemporary Control. PCC 2023. Lecture Notes in Networks and Systems*, Vol. 708, Springer, Cham, doi: [10.1007/978-3-031-35170-9_28](https://doi.org/10.1007/978-3-031-35170-9_28).
- AHSAN M., BISMOR D., MANZOOR M.A. (2023), ARL-Wavelet-BPF optimization using PSO algorithm for bearing fault diagnosis, *Archives of Control Sciences*, **33**(3): 589–606, doi: [10.24425/acs.2023.146961](https://doi.org/10.24425/acs.2023.146961).
- Analog Devices (n.d.), ADXL1002 Accelerometer Data-sheet. Analog Devices, Inc., <https://www.analog.com/en/products/adxl1002.html> (access: 2022).
- BISMOR D. (2019), Analysis and comparison of vibration signals from internal combustion engine acquired using piezoelectric and MEMS accelerometers, *Vibration in Physical Systems*, **30**(1): 2019112.
- DU C., JIANG F., DING K., LI F., YU F. (2021), Research on feature extraction method of engine misfire fault based on signal sparse decomposition, *Shock and Vibration*, doi: [10.1155/2021/6650932](https://doi.org/10.1155/2021/6650932).
- FIRMINO J.L., NETO J.M., OLIVEIRA A.G., SILVA J.C., MISHINA K.V., RODRIGUES M.C. (2021), Misfire detection of an internal combustion engine based on vibration and acoustic analysis, *Journal of the Brazilian Society of Mechanical Sciences and Engineering*, **43**: 336, doi: [10.1007/s40430-021-03052-y](https://doi.org/10.1007/s40430-021-03052-y).
- GÜL M., KARAER M., DOĞAN A. (2021), Design of piezoelectric acceleration sensor for automobile applications, *International Journal of Automotive Science And Technology*, **5**(4): 398–403, doi: [10.30939/ijastech..1006197](https://doi.org/10.30939/ijastech..1006197).
- HMIDA A., HAMMAMI A., CHAARI F., AMAR M.B., HADDAR M. (2021), Effects of misfire on the dynamic behavior of gasoline Engine Crankshafts, *Engineering Failure Analysis*, **121**: 1–19, doi: [10.1016/j.engfailanal.2020.105149](https://doi.org/10.1016/j.engfailanal.2020.105149).
- KUMANO K., AKAGI Y., MATOHARA S., UCHISE Y., YAMASAKI Y. (2020), Using an ion-current sensor integrated in the ignition system to detect precursory phenomenon of pre-ignition in gasoline engines, *Applied Energy*, **275**: 115341, doi: [10.1016/j.apenergy.2020.115341](https://doi.org/10.1016/j.apenergy.2020.115341).
- LI S., ZHANG Y., WANG L., XUE J., JIN J., YU D. (2020), A CEEMD method for diesel engine misfire fault diagnosis based on vibration signals, [in:] *2020*

- 39th Chinese Control Conference (CCC), pp. 6572–6577, doi: [10.23919/CCC50068.2020.9189312](https://doi.org/10.23919/CCC50068.2020.9189312).
12. LIN H.-C., YE Y.-C. (2019), Reviews of bearing vibration measurement using fast Fourier transform and enhanced fast Fourier transform algorithms, *Advances in Mechanical Engineering*, **11**(1): 1–12, doi: [10.1177/1687814018816751](https://doi.org/10.1177/1687814018816751).
 13. LIU X., SHI G., LIU W. (2021), An improved empirical mode decomposition method for vibration signal, *Wireless Communications and Mobile Computing*, pp. 1–8, doi: [10.1155/2021/5525270](https://doi.org/10.1155/2021/5525270).
 14. NAVEEN VENKATESH S. *et al.* (2022), Misfire detection in spark ignition engine using transfer learning, *Computational Intelligence and Neuroscience*, pp. 1–13, doi: [10.1155/2022/7606896](https://doi.org/10.1155/2022/7606896).
 15. ROSSI A., BOCCHETTA G., BOTTA F., SCORZA A. (2023), Accuracy characterization of a MEMS accelerometer for vibration monitoring in a rotating framework, *Applied Sciences*, **13**(8): 5070, doi: [10.3390/app13085070](https://doi.org/10.3390/app13085070).
 16. SHARMA A., SUGUMARAN V., BABU DEVA SENAPATI S. (2014), Misfire detection in an IC engine using vibration signal and decision tree algorithms, *Measurement*, **50**: 370–380, doi: [10.1016/j.measurement.2014.01.018](https://doi.org/10.1016/j.measurement.2014.01.018).
 17. SYTA A., CZARNIGOWSKI J., JAKLIŃSKI P. (2021), Detection of cylinder misfire in an aircraft engine using linear and non-linear signal analysis, *Measurement*, **174**: 108982, doi: [10.1016/j.measurement.2021.108982](https://doi.org/10.1016/j.measurement.2021.108982).
 18. TAMURA M., SAITO H., MURATA Y., KOKUBU K., MORIMOTO S. (2011), Misfire detection on internal combustion engines using exhaust gas temperature with low sampling rate, *Applied Thermal Engineering*, **31**(17–18): 4125–4131, doi: [10.1016/j.applthermaleng.2011.08.026](https://doi.org/10.1016/j.applthermaleng.2011.08.026).
 19. TAO J., QIN C., LI W., LIU C. (2019), Intelligent fault diagnosis of diesel engines via extreme gradient boosting and high-accuracy time-frequency information of vibration signals, *Sensors*, **19**(15): 3280, doi: [10.3390/s19153280](https://doi.org/10.3390/s19153280).
 20. WANG J. *et al.* (2022), Misfire and knock detection based on the ion current inside a passive pre-chamber of gasoline engine, *Fuel*, **311**: 122528, doi: [10.1016/j.fuel.2021.122528](https://doi.org/10.1016/j.fuel.2021.122528).
 21. YAŞAR A., KESKIN A., YILDIZHAN S., ULUDAMAR E. (2019), Emission and vibration analysis of diesel engine fuelled diesel fuel containing metallic based nanoparticles, *Fuel*, **239**: 1224–1230, doi: [10.1016/j.fuel.2018.11.113](https://doi.org/10.1016/j.fuel.2018.11.113).
 22. ZHOU H., MENG S., HAN Z. (2023), Combustion characteristics and misfire mechanism of a passive pre-chamber direct-injection gasoline engine, *Fuel*, **352**: 129067, doi: [10.1016/j.fuel.2023.129067](https://doi.org/10.1016/j.fuel.2023.129067).